PNAS RESEARCH ARTICLE | EARTH, ATMOSPHERIC, AND PLANETARY SCIENCES
ANTHROPOLOGY

Exploring geomagnetic variations in ancient mesopotamia: Archaeomagnetic study of inscribed bricks from the 3rd–1st millennia BCE

Matthew D. Howland[a,b,1], Lisa Tauxe[c,1], Shai Gordin[d,e], Mark Altaweel[f], Brendan Cych[g], and Erez Ben-Yosef[b]

Contributed by Lisa Tauxe; received August 3, 2023; accepted November 3, 2023; reviewed by Florian Lhuillier and Martin Worthington

This study presents 32 high-resolution geomagnetic intensity data points from Mesopotamia, spanning the 3rd to the 1st millennia BCE. These data contribute to rectifying geographic disparities in the resolution of the global archaeointensity curve that have hampered our understanding of geomagnetic field dynamics and the viability of applying archaeomagnetism as a method of absolute dating of archaeological objects. A lack of precise and well-dated intensity data in the region has also limited our ability to identify short-term fluctuations in the geomagnetic field, such as the Levantine Iron Age geomagnetic Anomaly (LIAA), a period of high field intensity from ca. 1050 to 550 BCE. This phenomenon has hitherto not been well-demonstrated in Mesopotamia, contrary to predictions from regional geomagnetic models. To address these issues, this study presents precise archaeomagnetic results from 32 inscribed baked bricks, tightly dated to the reigns of 12 Mesopotamian kings through interpretation of their inscriptions. Results confirm the presence of the high field values of the LIAA in Mesopotamia during the first millennium BCE and drastically increase the resolution of the archaeointensity curve for the 3rd–1st millennia BCE. This research establishes a baseline for the use of archaeomagnetic analysis as an absolute dating technique for archaeological materials from Mesopotamia.

mesopotamia | archaeomagnetism | archaeology | chronology | archaeomagnetic dating

Significance

Reconstructing the behavior of Earth's magnetic field during archaeological periods is crucial for both achieving a better understanding of the field and related natural phenomena and for providing a basis for absolute dating archaeological materials. Here, we analyzed inscribed baked bricks from Mesopotamia from the 3rd–1st millennia BCE, which are well-dated based on their association with well-known regional kings. Providing well-dated and highly precise archaeomagnetic intensity data for the region, our results 1) demonstrate the potential of this archaeomagnetic analysis of baked bricks; 2) facilitate a better understanding of the field, including insights regarding the Levantine Iron Age geomagnetic Anomaly; and 3) provide a basis for archaeomagnetic dating in a key region in the history of complex societies.

Paleomagnetic research aims to reconstruct the direction and intensity of the geomagnetic field over time, most commonly by the examination of thermoremanent magnetization (TRM) recorded in iron oxide minerals within materials when they are heated to high temperature and then cooled in a magnetic field (1). The conditions of Earth's magnetic field at the time of cooling can be approximated based on approaches pioneered by Thellier (2) and Koenigsberger (3). Generally, examination of the geomagnetic field consists of the study of its intensity and direction—the latter measured in angles of inclination and declination. Identifying field conditions in the Holocene generally requires examination of archaeological materials, allowing for the development of high-resolution models that can reconstruct variations in the geomagnetic field occurring over brief time scales (i.e., decades to centuries), known as secular variation. Study of archaeological materials can provide data allowing for the reconstruction of both the intensity (4) and direction (5) of Earth's magnetic field. Directional studies, however, require that the exact orientation of archaeological objects when TRM was acquired at cooling to be preserved through excavation and laboratory analysis. As such, many analyses, including the present study, focus solely on the collection of archaeointensity data when the orientation of samples during TRM acquisition is unknown. Still, whether leveraging data related to intensity and/or direction (and ideally both), paleomagnetic research contributes to the viability of absolute dating of archaeological materials through archaeomagnetic analysis (4). Much research has been dedicated to the establishment of geomagnetic secular variation models (6–8) and archaeointensity curves (9, 10) based on archaeological data. Construction of these models requires highly precise and well-dated samples in order to identify short-term variations (e.g., high field "spikes"; 11, 12) in the geomagnetic field. Archaeomagnetic material must be analyzed according to validated experimental protocols (e.g., ref. 13) and pass rigorous specimen selection criteria (e.g., ref. 14) in order to meet established precision standards (10) for inclusion in high-quality models of secular variation of archaeointensity. Moreover, archaeomagnetic samples are generally plagued by chronological uncertainty in the range of hundreds of years—only ca. 30% of published samples have an age range of ≤50 y (15). Only tightly dated samples such as these are viable for improving the quality of archaeointensity curve reconstruction (16).

However, the availability of such high-quality intensity data is subject to geographic disparities, limiting our ability to reconstruct global high-resolution archaeointensity curves. Scarcity of precisely calibrated and dated archaeomagnetic intensity data is especially

Author contributions: M.D.H., L.T., and E.B.-Y. designed research; M.D.H., L.T., S.G., M.A., and E.B.-Y. performed research; B.C. contributed new reagents/analytic tools; M.D.H., L.T., S.G., B.C., and E.B.-Y. analyzed data; and M.D.H., L.T., M.A., S.G., and E.B.-Y. wrote the paper.

Reviewers: F.L., Ludwig-Maximilians-Universitat Munchen; and M.W., The University of Dublin Trinity College.

The authors declare no competing interest.

[1]To whom correspondence may be addressed. Email: mdh5169@gmail.com or ltauxe@ucsd.edu.

This article contains supporting information online at https://www.pnas.org/lookup/suppl/doi:10.1073/pnas.2313361120/-/DCSupplemental.

Published December 18, 2023.

evident in Mesopotamia (composed of present-day Iraq and parts of Syria, Turkey, Iran, and Kuwait) for the 3rd–1st millennia BCE, a highly significant region and time period for the development of urbanism and social complexity. Though Northern Mesopotamia (Eastern Syria, Southeastern Turkey, and Northern Iraq) is well represented by 79 high-quality data points (17–24), Southern Mesopotamia (Southern Iraq, Kuwait, and Southwestern Iran) is underrepresented, with only 25 data points from four projects (18, 25–27; Fig. 1)—an average of only one data point per 120 y. This sampling density is not sufficient to reconstruct archaeomagnetic spikes, which may occur within a century (10). Furthermore, the few published results from Southern Mesopotamia generally lack both tight chronological control and precise measurements of the intensity of Earth's magnetic field and therefore have limited usefulness for reconstructing secular variation of intensity in the region. By contrast, the Southern Levant is well-populated with archaeointensity data from the 3rd–1st millennia BCE, with over 150 data points from a range of projects representing this region (4, 9–12, 16, 28, 29, among many others; Fig. 1)—an average of 1 per 20 y. The detail of this assemblage and the quality of its constituent data have enabled the development of the Levantine Archaeomagnetic Curve (LAC; 8, 9, 12), a high-resolution geomagnetic intensity curve for the Levant and Northern Mesopotamia. The LAC, in turn, has facilitated the discovery of a localized period of geomagnetic spikes from ca. 1050 to 550 BCE, consisting of extremely high-intensity values—virtual axial dipole moments (VADMs; 30) higher than 160 ZAm^2—and rapid changes in Earth's magnetic field, now known as the Levantine Iron Age geomagnetic Anomaly, (LIAA, 10–12). Recent research has corroborated the existence of the high-intensity values (above 150 ZAm^2) of the LIAA as far as Turkey (29), Georgia (31), Bulgaria (32), Italy and Greece (33), Spain (8, 34, 35), the Canary Islands (36), the Azores (37), and China (38). Based on this evidence, the question of the geographical extent and spread over time of the LIAA has been the subject of discussion and debate (6, 8, 10, 12, 32, 39, 40).

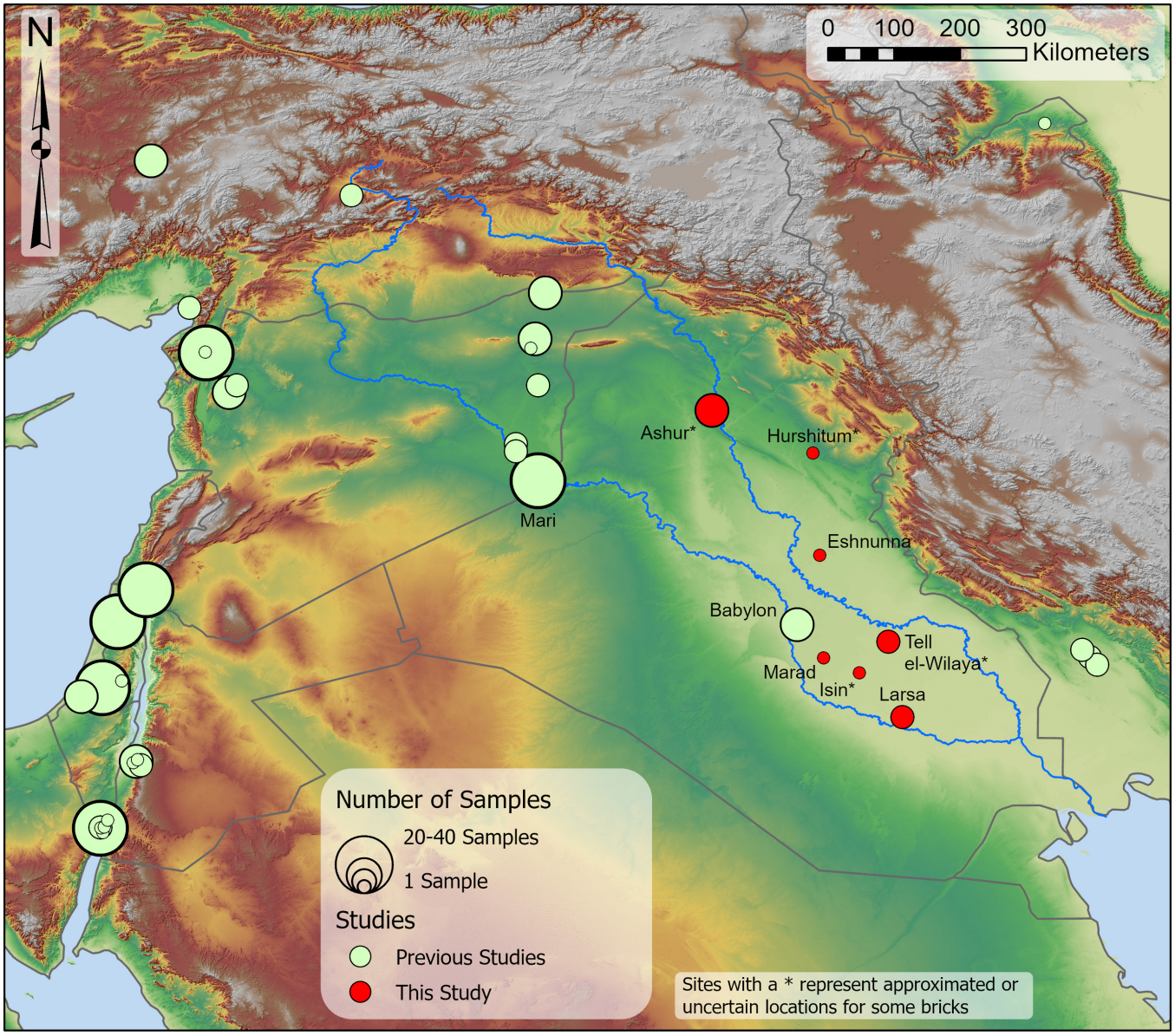

Fig. 1. Regional map of the Levant and Mesopotamia, illustrating the locations of high-quality archaeointensity samples from previous studies and this study. Only samples measured according to validated experimental protocols (e.g., ref. 13) are shown. The historical region of Mesopotamia generally consists of the region between and surrounding the Tigris and Euphrates Rivers, depicted here.

Yet, research on the LIAA in Mesopotamia lags due to the geographic disparities described above. Prior to recent work on Mesopotamian baked bricks, only 11 intensity data points from the period of the LIAA had been published from the entirety of Mesopotamia: three archaeological baked bricks and three potsherds from Iraq (27), three baked bricks and one potsherd from Syria (19, 20), and one burnt mud brick from Turkey (18). Most recently, five baked bricks from the Ishtar Gate from Babylon in Iraq have been added to this assemblage (41). While the materials from Northern Mesopotamia (Syria and Turkey) feature relatively high values (averaging ca. 141.5 ZAm^2), the materials from Iraq [published by Walton (27)] average only ca. 99.1 ZAm^2, well below the range of values from samples on the basis of which the LIAA has been identified (often above 150 ZAm^2). As such, the LIAA has not been conclusively demonstrated in Southern Mesopotamia. These results contradict recent regional and global models of the geomagnetic field during this period (10, 39–40), which clearly indicate that the high intensity of the LIAA should be expected to be seen across Mesopotamia as a whole. This inconsistency must be addressed through further experimentation, which could either confirm the results of Walton (27) and indicate that the LIAA did not extend to Mesopotamia during the early-mid 1st millennium BCE or, alternatively, demonstrate the high values of the LIAA with the type of precise and tightly dated samples that are needed to construct regional and global models (10, 40–42). Regardless, the results of Walton (27) call into question the geographic extent of the LIAA and whether Mesopotamia as a whole, and Southern Mesopotamia in particular, experienced high geomagnetic intensities from ca. 1050 to 550 BCE.

The extent to which the high VADM values that are associated with the LIAA can be observed in late-second and first-millennium archaeomagnetic samples from these regions is therefore a pressing question for understanding Earth's magnetic field during this period. More broadly, a lack of published data for the 3rd-1st millennia BCE in Mesopotamia hampers efforts to develop localized models of secular variation of intensity at high resolution and, as such, limits our ability to apply archaeomagnetic analysis as a technique of absolute dating. This latter drawback is especially significant given the importance of Mesopotamian archaeological sites in understanding the development of early states and urbanism (43, 44) and the persistence of chronological uncertainties that plague the archaeology of the region (45). Only high-resolution archaeomagnetic analysis of precisely dated samples is suited to address these challenges.

Baked brick—mud bricks that have been fired in a kiln—offer a potential solution to the challenges of reconstructing ancient archaeointensity curves for Mesopotamia. Mud bricks were a commonly used construction material across ancient Mesopotamia and beyond for millennia across a range of contexts (46). Mud bricks were generally made from a mix of earth, chopped straw, and water, and shoveled into a mold before being left to dry in the sun (47). Importantly, bricks were also sometimes kiln-fired in antiquity (only baked bricks can be used for archaeomagnetic purposes). Baked bricks are seen in the archaeological record of Mesopotamia as early as the 5th millennium BCE and were used for specialized purposes by the 4th millennium BCE (at Uruk, 48); they became increasingly common and standardized in shape by the end of the 3rd millennium BCE (49).

The process for making baked bricks in Mesopotamia required high-temperature firing, likely using scarce wood or occasionally bitumen (a semisolid form of petroleum that was used for protection against moisture, as mortar, and sometimes as fuel) to reach temperatures of over 600 °C in (likely closed) kilns (49). The expenses associated with baking bricks meant that these objects were typically limited to specific, often elite, buildings such as temples, palaces, and sometimes parts of private homes, particularly private residences of the wealthy (46, 50). Fired bricks were also generally reserved for areas needing an extra level of resistance against erosion, including dikes, embankments, drains, water basins, and channels, facing lower courses of walls, and for paving floors and door sockets (48, 51–52). These contexts called for increased durability given the tendency of sun-dried mud brick to quickly degrade in wet or high-traffic conditions. Baked bricks may be found in situ or removed from their original context, as these objects were often reused in antiquity and even in recent periods due to their durability and the relatively high cost of manufacturing new bricks.

Fig. 2. Brick B533 from the Slemani Museum. This baked brick dates to the reign of Nebuchadnezzar II (ca. 604 to 562 BCE) based on the interpretation of the inscription. This object was looted from its original context before being acquired by the Slemani Museum and stored in that museum with agreement from the central government.

Baked bricks from Mesopotamia have been subjected to archaeomagnetic analyses in several studies (17–21, 23, 27), although in archaeomagnetic projects, the use of other materials such as ceramics and hearth fragments is more common—only ca. 32% of artifacts sampled previously for archaeomagnetic analysis from present-day Iraq or Syria from the 3rd–1st millennia BCE have been bricks (15). However, baked bricks provide an ideal target for archaeomagnetic sampling since many such bricks (see example in Fig. 2) feature stamped or inscribed inscriptions in Sumerian or Akkadian, enabling these artifacts to be precisely dated to the reigns of individual Mesopotamian kings whose names often adorn the bricks (53). Inscriptions were usually placed on bricks either using stamps or, more rarely, direct writing prior to firing in kilns. Bricks may also be dated based on size and shape, relying on the standardization of bricks to different sizes in different periods, although this is not as reliable or as tight as the use of inscriptions (54). These factors even enable the dating of bricks found in secondary contexts. Clay cones, used for architectural purposes and also often stamped with royal inscriptions (54), provide similar potential for sampling. The relatively tight date ranges of

individual kings provide a more precise basis for absolute dating of archaeomagnetic samples than does, for example, an archaeological stratum dated by radiocarbon. Dating these artifacts to the reign of a particular king allows for a resolution of years or, at the most, decades, rather than up to 200 y or more, depending on radiocarbon probabilities. Dating bricks on the basis of epigraphy can, therefore, improve the chronological resolution of archaeomagnetic samples. One caveat to this advantage is that the absolute chronology of early 3rd and 2nd millennium BCE Mesopotamian kings is unsettled (55–61), with uncertainty of up to 150 y in the absolute dates of individual kings. Here, we apply the Low Chronology (58), which results in the best agreement between our data and the LAC among the various chronologies proposed. These debates do not apply in the first millennium BCE, where historical and archaeological evidence has resulted in a more exact understanding of the absolute dates of the reigns of Mesopotamian kings (61). Moreover, archaeomagnetic intensity data can contribute toward the resolution of chronological uncertainty, which would drastically improve the precision of samples from the early 3rd and 2nd millennium BCE. Ultimately, the use of inscribed bricks for archaeomagnetic analyses provides a basis for more precise dating of intensity samples (assuming chronological issues can be resolved), improving the temporal resolution of intensity curves and allowing for the identification of short-term spikes in the geomagnetic field.

Results

The assemblage of artifacts for this project consists of 139 fired and inscribed clay objects, including 120 bricks from the Slemani Museum in Iraqi Kurdistan (62), 16 baked bricks and two clay cones from the Yale Babylonian Collection (YBC), and one baked brick from Marad, via recent al-Qadisiyah University excavations. Artifacts from the Slemani Museum and the YBC lack clear provenience—YBC objects were acquired from private collections prior to 1970 while bricks from the Slemani Museum were looted from archaeological sites in Iraq but are nevertheless the legitimate cultural property of the Iraqi government and curated by the museum under granted permission from the central government as part of the objects' repatriation. Of the 139 objects, 40 were chosen for initial archaeomagnetic study based on characteristics including legibility of inscription and range of chronology (Dataset S1). Other bricks were reserved for follow-up study. Each of the 40 bricks sampled is inscribed; these inscriptions allow 38 of the 40 bricks to be dated to the reign of an individual king (periods of ≤50 y) and for the original provenience of each object to be estimated (Dataset S1 and Fig. 2). Orthophotographic images of each of the sampled objects is available online https://github.com/DigitalPasts/BricksGeomagnetism.

The 40 objects range from the late 3rd millennium to the mid-1st millennium BCE. The assemblage includes bricks from the reigns of 12 kings, including nine bricks likely looted from quay walls constructed by Adad-Nirari I [63 (Royal Inscriptions of Mesopotamia, Assyrian Periods; RIMA 1): A.0.76.9-10] at Ashur (64), as well as bricks inscribed with the names of well-known Mesopotamian kings including Nebuchadnezzar II, Shulgi, and Tukulti-Ninurta I. Brick B980 features a heretofore unparalleled inscription of Iakūn-dīri, son of Sumanim, a king of Hurshitum previously only known from a seal of his servant Iamūt-Kuluh [65 (Royal Inscriptions of Mesopotamia, Early Periods; RIME): E4.0.11]. Two bricks (B988 and B989) were only able to be affiliated with the Middle Assyrian (ca. 1363 to 912 BCE)/Neo-Assyrian (911 to 609 BCE) periods, rather than an individual king, and were subsequently excluded from the study due to a lack of chronological resolution. In general, the baked bricks range in date and original geographic and archaeological context. The varied origins of the bricks and different clay materials do not impact their ability to record and store information about Earth's magnetic field. In most cases, these bricks can be associated with specific archaeological sites in both Northern and Southern Mesopotamia, including Ashur, Eshnunna, Isin, Ur, Larsa, Tell el-Wilaya, and Marad.

Overall, 263 specimens from the 40 objects (archaeomagnetic samples) were subjected to the IZZI paleointensity experiment of Yu et al. (13) with cooling rate and anisotropy corrections (resulting in a decrease in specimen dispersion per sample and an average ~7.8% reduction in SD) and analyzed using the Bias Corrected Estimation of Paleointensity (BiCEP) method (41, 66). Of the 40 objects, 34 passed the acceptance criteria for successful results with BiCEP correction (Dataset S2) and the additional acceptance criteria. Five objects failed as there were fewer than five successful specimens, while one failed the acceptance criteria of a 95% confidence spread of greater than 16 μT, or when converted to the equivalent 1 sigma value (by dividing by 4), greater than 10% of the intensity. Two of the 34 objects (bricks B988 and B989) were subsequently removed from consideration in the study due to a lack of tight chronological control (i.e., dating to the Middle Assyrian or Neo-Assyrian periods rather than the reign of an individual king) but are included in supplementary material and discussion. Arai plots for two representative successful specimens and one unsuccessful specimen are illustrated in Fig. 3 *A*–*C*. BiCEP plots for two objects passing and one object not passing additional acceptance criteria are illustrated in Fig. 3 *D*–*F*, respectively.

The median estimate for the archaeointensity of each of the 32 baked bricks is plotted in Fig. 4*A* along with the intensity values of each successful specimen. Results were not averaged by king as the objects sampled were not necessarily manufactured contemporaneously, even when associated with the reign of the same king. Thus, variations in observed intensity over the reign of an individual king may relate to either experimental uncertainty or actual secular variation. Sample median estimates are plotted against the LAC (10–12) in Fig. 4*B*, along with previously published data from Mesopotamia. The age ranges along the *X* axis provided for each sample represent the length of the reign of the king (or dynasty) that each baked brick has been associated with on the basis of inscriptions. Absolute dating of the 2nd and 3rd millennium BCE bricks is according to the Low Chronology (58), which results in the best agreement between our data and the LAC. Error bars on the *Y* axis reflect the Bayesian uncertainties derived from the BiCEP method, comparable to the 2σ extended error bars of Shaar and Tauxe (14).

Discussion

The 32 bricks analyzed here represent a major addition to the archaeomagnetic assemblage from Northern and Southern Mesopotamia in the 3rd–1st millennia BCE, providing geomagnetic intensity data from several major sites in this region for the first time. These findings contribute to increasing the resolution of the geomagnetic intensity curve for Mesopotamia as a whole during this period. Results from this study, though largely compatible with previously published intensity values, notably differ from published results during the first millennium BCE (Fig. 4*B*). This period carries outsized significance in paleomagnetic research given the dramatic archaeomagnetic spikes of the LIAA. The ten baked bricks dating to the LIAA period (ca. 1050 to 550 BCE) from the present study—all but one from Southern Mesopotamian sites and averaging ca. 138.3 ZAm^2—contrast sharply with the

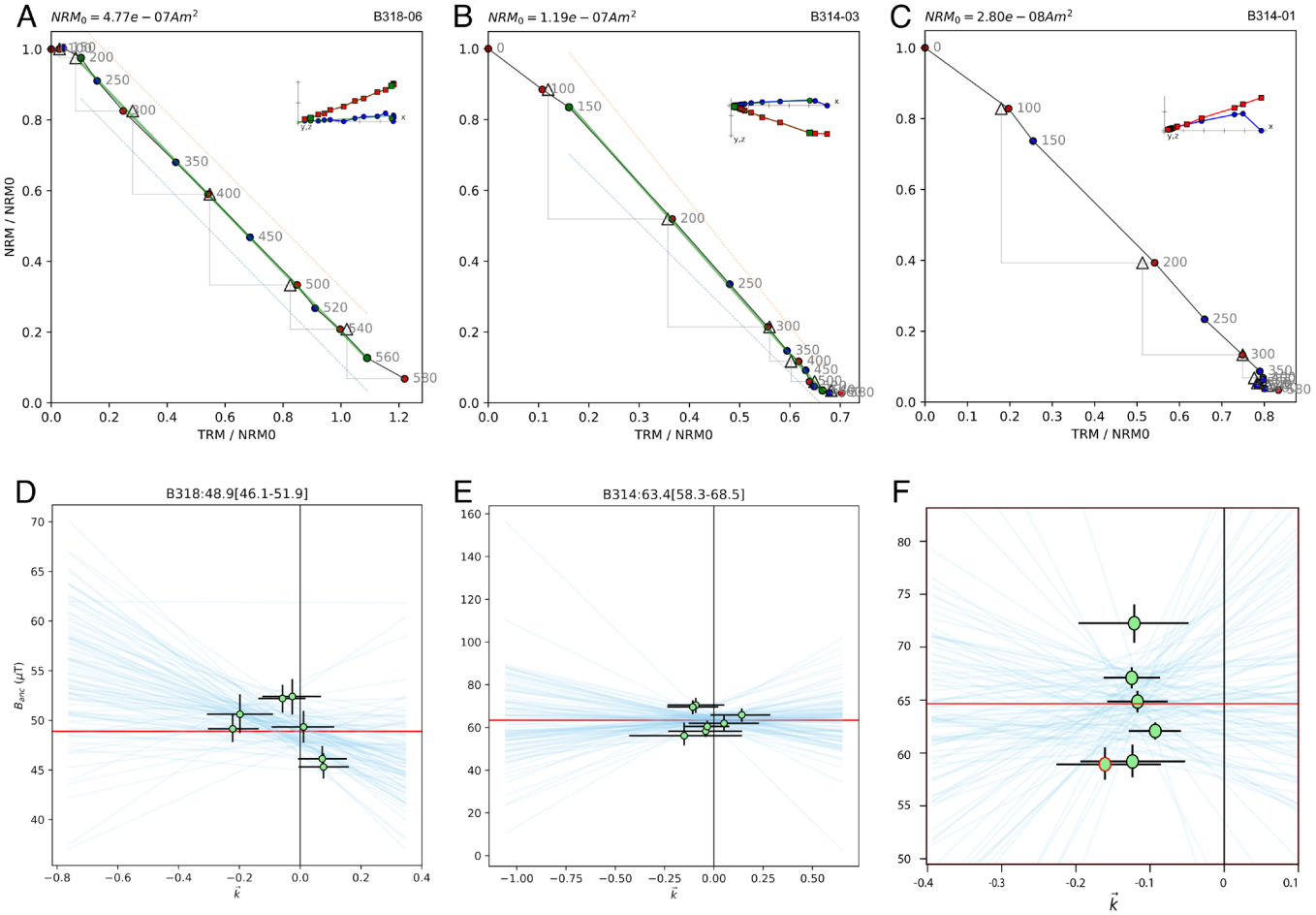

Fig. 3. Representative Arai and BiCEP plots from the analysis. Arai plots are shown for successful specimens (*A*) B318-06 and (*B*) B314-03 and for unsuccessful specimen (*C*) B314-01. Zijderveld diagrams for these specimens are illustrated in the upper right corner of each plot. BiCEP plots are shown for objects (*D*) B318 and (*E*) B314, passing acceptance criteria, and (*F*) B562, failing acceptance criteria. Intensity of each specimen is plotted against Arai plot curvature criterion ($\vec{k}$; 65). In BiCEP, median estimates for each object are calculated by the average y-intercept of best-fit lines of intensity and curvature of Arai plots for each specimen. Object B562 is rejected on the basis of a maximum estimated intensity spread greater than 16.0 μT and 10% of B_{anc} (illustrated by the range of blue lines at the y-intercept).

three baked bricks and three potsherds previously published by Walton (27), which average ca. 99.1 ZAm^2. Similarly, bricks from the period of the LIAA from the present study contrast with the bricks from earlier periods, which average ca. 101.3 ZAm^2. As such, the results from the present study, unlike those of Walton (27), are consistent with the aggregated results of the LAC and suggest that high geomagnetic intensity values during the late second and early first millennium BCE were not limited to the Levant, Syria, and many other parts of the world, but rather also occurred in all parts of Mesopotamia. Thus, these findings corroborate the limited results that have demonstrated high values for Northern Mesopotamia during the period of the LIAA (18–20) and recent results demonstrating high values in Southern Mesopotamia during the latest part of the LIAA (40). Our work suggests that the results of Walton (27) should be reevaluated in light of new developments in our understanding of the intensity of Earth's magnetic field in the first millennium BCE.

Our results from the second and third millennia BCE are broadly consistent with both the assemblage of previously published intensity data from Mesopotamia (17–27, 41) and the LAC curve (9; Fig. 4*B*), with two irregularities. One brick, Y018, associated with Ur-Ningishzida, a governor of Eshnunna from the 20th century BCE, features lower intensity values than observed in the LAC. However, this brick is not entirely inconsistent with data from Iraq published by Aitken (20; Fig. 4*B*). Similarly, one near-identically dated sample group (S-3) from Tel Megiddo published by Shaar (9) also lies below the 95% CI of the curve. These results, therefore, suggest a need for further investigation of a potential intensity minimum at ca. 1950–1900 BCE. Brick B980, associated with the previously unknown king Iakūn-dīri of Hurshitum, also falls outside the CI of the LAC at its lowest point. In general, though the LAC is well-populated with data during certain periods, the curve suffers from a relative scarcity of tightly dated samples from a few periods, including the mid-late 3rd millennium BCE and the mid-late 2nd millennium BCE. Our data help contribute to increasing the resolution of the curve during these key periods for the LAC in general as well as contributing to the archaeointensity curve for Mesopotamia specifically.

The observation of high values consistent with the LIAA in bricks from Iraq also has functional value for future archaeomagnetic dating. The geomagnetic field intensity high values of the LIAA, ranging from ca. 120 ZAm^2 to upward of 150 ZAm^2, have been shown to be a clear chronological indicator of the period of this geomagnetic anomaly in other regions. Our results, in combination with those of Gallet (19, 20), Ertepinar (18), and Di Chiara (41), show that high archaeointensity values (i.e., values at or above ca. 130 ZAm^2) can likewise be used to date archaeological artifacts to the period between ca. 1050 and 550 BCE across Mesopotamia, in both northern and southern regions. For example, Bricks B988 and B989 in our study cannot be associated with

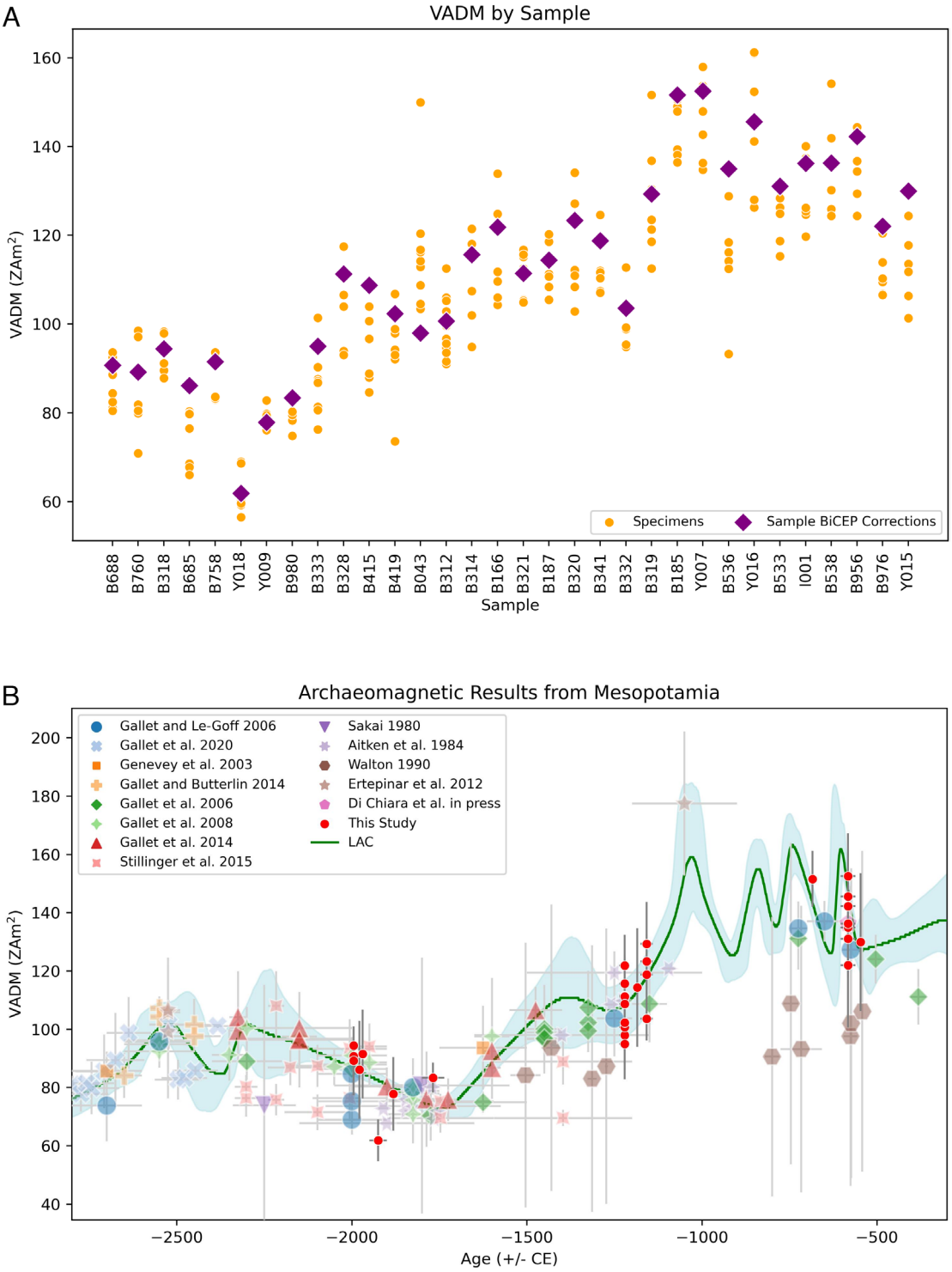

Fig. 4. VADM values for objects and individual specimens (*A*) and object results plotted against the LAC (*B*; 10). Each of the 32 baked bricks and that passed acceptance and chronological criteria in this study are depicted in (*A*), along with VADM values for the specimens for each object. In some cases, the BiCEP correction method results in an intensity value that is higher or lower than the specimen results, based on Arai plot curvature-based correction (65). (*B*) depicts the 32 baked bricks that passed acceptance and chronological criteria in this study and results from previous studies from Mesopotamia (data from GEOMAGIA50.v3, 15), plotted against the LAC (10). Results are illustrated with extended error bars (effectively 2σ) for intensity values (*Y* axis) and error depicting the range of potential ages for each object, based on the interpretation of the inscription. Dates for the present study are according to the Low Chronology (58).

a specific king on the basis of epigraphy and must be dated broadly to the Middle or Neo-Assyrian periods (ca. 1363 to 609 BCE). However, since these objects feature high-intensity values (VADMs averaging ca. 142.4 ZAm^2) that only occur during the limited time frame of the LIAA, these bricks can be associated with the period of the LIAA that overlaps with these historical periods (i.e., ca. 1050 to 609 BCE). This narrowing of the dates of these bricks serves as a small illustration of the utility of developing the archaeomagnetic curve and understanding secular variation in Mesopotamia for the purposes of absolute dating. Future work to further refine and increase the resolution of the intensity curve for Southern Mesopotamia can improve the prospects for the use of archaeomagnetic dating on uninscribed material from this region with greater precision. Moreover, further experimentation on

establishing a paleodirectional curve for this period (e.g., ref. 5) would improve the prospects of the use of archaeomagnetic analysis as a dating technique even further.

These results also have implications for the ongoing, larger debate over the potential maximum intensity and rate of change of the geomagnetic field (10, 12, 31, 67). Recent studies examining the archaeointensity curve for the Eastern Mediterranean from well-dated samples have revealed four geomagnetic spikes (making up the LIAA) between 1050 and 550 BCE, with large field change rates greater than previously hypothesized were possible (10). Our five data points from the reign of Nebuchadnezzar II (604 to 562 BCE) display a wide range of intensity values from this short 42-y period, which may provide some corroboration of the rapid changes in geomagnetic field intensity during the last part of the LIAA. This variation may also be explained by experimental uncertainty, although it should be noted that the available data from Mesopotamia and the LAC do suggest a trend of rapid decrease in field intensity during the first half of the 6th century BCE, in aggregate. The results analyzed here from the reign of Nebuchadnezzar II also closely parallel the bricks from the era of the same king analyzed by Di Chiara et al. (41)—results from the eight bricks from the present study average 137.6 ZAm^2 while the five bricks from (41) average 136.0 ZAm^2.

From a broader perspective, this work further establishes the validity of applying archaeomagnetic methods to kiln-baked bricks (17–21, 23, 41). Though these bricks are often not suitable for directional analyses given that they are found in different contexts from those in which they acquired TRM, these materials provide an excellent and consistent basis for analysis of archaeointensity—231 of the 263 specimens that make up the 40 objects analyzed in this study would pass the experimentally verified automatic acceptance criteria of Shaar and Tauxe (14). Although the method is destructive, the amount of material needed for the experiment is minimal—we have found that a sample as small as 2g (ca. 1.0 cm^3) is sufficient for the magnetic experiments.

Dating baked bricks on the basis of inscriptions naming certain kings provides a relatively tight chronological margin for archaeomagnetic results, as discussed above. Though the wide range of chronologies tying the reigns of individual Mesopotamian kings to absolute dates is a complicating factor, future archaeomagnetic dating of bricks from the 2nd millennium BCE can complement the range of methodological approaches—dendrochronology, astronomical observation, epigraphic data, and radiocarbon dating—that have been applied to this question without fully resolving the issue (45). Archaeomagnetic approaches, including intensity and paleodirectional study, can help address this chronological impasse. In doing so, archaeomagnetic results from inscribed baked bricks should become increasingly valuable for establishing a tightly anchored intensity curve as additional evidence is brought to bear on the Mesopotamian chronological debate.

Materials and Methods

Samples were collected with agreement on site at the Slemani Museum in Iraqi Kurdistan, at the YBC in the United States, and one sample was provided by al-Qadisiyah University excavations. Baked brick inscriptions were recorded using image-based modeling in order to obtain a high-resolution orthophotograph for documentation and later interpretation. Each brick from the Slemani Museum was identified and associated with a particular king based on reading and decipherment of the cuneiform inscriptions. King associations for bricks (and two clay cones) collected from the YBC were derived from interpretations of brick inscriptions, which corresponded to existing interpretations in the catalog of the Yale Peabody Museum. Date ranges for each object were determined based on the reigns of Mesopotamian kings identified in these inscriptions, applying the Low Chronology where relevant (57). Detailed interpretations for each brick and YBC catalog numbers are presented in Dataset S1 and at https://github.com/DigitalPasts/BricksGeomagnetism.

Samples were obtained by carefully chipping fragments averaging ca. 2 g from the back or broken edges of bricks and brought back to the Scripps Institution of Oceanography Paleomagnetic Laboratory for archaeomagnetic experimentation.

Experiments were performed using the Paleomagnetic Laboratory's high-capacity low-thermal gradient oven and a 2G Enterprises DC SQUID three axis through-bore cryogenic magnetometer. Magnetic susceptibility was measured with a Bartington susceptibility bridge. In the laboratory, each sample (fragment of a brick) was broken into ca. 100 mg specimens and glued into borosilicate glass specimen tubes with a fiducial line and a laboratory specimen identification number using a high-temperature, low magnetic moment glue (KaSil). These specimens were subjected to the IZZI paleointensity experiment (13), a modification of the original Thellier-Thellier method (68). Directional study was not conducted due to uncertainty regarding the orientation of the objects at the time when they acquired TRM. In this protocol, specimens are heated to progressively higher temperatures and cooled in applied laboratory fields (I steps) or in zero field steps (Z steps), with the order of these cooling fields (IZ or ZI) alternating at each temperature step. A lower temperature, in-field step is also performed after each IZ step to monitor the potential of specimens to acquire partial thermal remanence (69). Stepwise heating continues until at least 90% of the natural remanent magnetization (NRM) is removed in zero field steps. At the conclusion of this experiment, the ratio of the NRM lost in zero-field steps to the TRM gained in in-field steps should match the ratio of the ancient geomagnetic field to the applied laboratory field, under ideal conditions.

Thermal demagnetization through the IZZI protocol was carried out in temperature stages increasing by 50 °C from 100 °C to 500 °C and by 20 °C from 500 °C to 580 °C at lab fields of 40 microtesla for one experiment and 60 microtesla for a second experiment. Cooling rate experiments were conducted on all specimens and consisted of three steps at 580 °C–a fan-cooled step (average cooling rate of ca. 0.31 °C per second), a slow-cooled step (average cooling rate of ca. 56 °C per hour), and a second fan-cooled rate to check alteration. An average cooling rate correction of 1.007826 was applied based on results from these experiments. Anisotropy experiments were also conducted on every specimen, consisting of a demagnetization step, six TRM acquisition steps at orthogonal orientations (+x, −x, +y, −y, +z, −z), and an alteration check step. Due to degradation of the specimen glue during anisotropy experiments, specimen anisotropy results that displayed circular SD results greater than 2.0 on any in-field step were discarded. Based on 200 specimens with successful anisotropy experiments, an average correction of 0.979565 was applied. The application of these corrections led to a reduction in the dispersion of specimens, resulting in an average ~7.8% decrease in the SD of archaeointensity measurements per sample. Datasets resulting from these analyses were analyzed using the PmagPy software package (70) and the BiCEP (66) technique, which provides a basis for the interpretation of paleomagnetic specimens that do not fully conform to uniaxial single domain grain theory (1) that is fundamental to archaeomagnetic experiments. The BiCEP method assumes that deviation from ideal conditions occurs on a continuum, and as specimens' behavior becomes more nonideal, paleointensities become more biased and Arai plots become less linear (66; however, note that other factors can also cause curvature of Arai plots, e.g., ref. 71). Nonideal specimens can therefore be used for the estimation of unbiased paleointensity based on the curvature of their Arai plots rather than rejected by traditional binary specimen selection criteria (e.g., ref. 14). A fuller explanation of the value of this method can be found in refs. 40 and 66. In addition to BiCEP correction, two acceptance criteria were added at the level of the archaeomagnetic sample (i.e., baked brick): a minimum of five successful specimens and a maximum spread between minimum and maximum sample intensity of 16 μT (equivalent to extended error bars of $\mp 1\sigma$, 4μT; cf. 14,64) according to BiCEP estimates. An exception was made for specimens that failed this criterion if the spread divided by a factor of 4 times the average intensity was less than 10% of the average intensity. These criteria are consistent with those used in the CCRIT criteria of ref. 14.

A small adjustment to the prior of the BiCEP correction was made: The "c" parameter (the slope of the line relating paleointensity bias and curvature) was given a prior of a Cauchy distribution with location zero and scale 20, which was derived from the distribution of paleointensities and curvatures in the test dataset of ref. 72. If all specimens in a site cluster with a small range of paleointensity values and curvatures (as is seen in e.g., Fig. 3*F*), a line with almost any slope could

be driven through the points, leading to a large uncertainty in the BiCEP estimate. We expect that specimens with a small absolute curvature will have little bias, and so the revised prior restricts the available fitting lines to reduce the probability of extremely steep slopes (which would imply large bias at small curvature). Our revised prior improves the precision of BiCEP estimates for sites with a small number of high quality (very low curvature) paleointensity specimens. It has a negligible effect on sites with large numbers of specimens, or with a wider range of curvatures, where a line fit can more easily be made.

Data, Materials, and Software Availability. Code used to analyze the data is available in https://github.com/PmagPy/PmagPy (73) and https://github.com/bcych/BiCEP_GUI (74). On acceptance of the manuscript, archaeomagnetic data will be made public at: https://earthref.org/MagIC/19893 (75). Orthophotographs of sampled bricks are available at https://github.com/DigitalPasts/BricksGeomagnetism (76). For the purposes of review, the archaeomagnetic data are available at: https://earthref.org/MagIC/19893/d4b397b9-f200-479f-8cbf-1492e3df910b (77).

ACKNOWLEDGMENTS. We thank Agnete Lassen, Klaus Wagensonner, Christeanne Santos, Jeffrey Gee, Yoav Vaknin, and Ron Shaar for discussions and support. We would like to thank the manuscript reviewers, F.L. and M.W., for taking the time and effort necessary to review the manuscript. We sincerely appreciate all valuable comments and suggestions, which helped us to improve the quality of the manuscript. This study was financially supported by United States–Israel Binational Science Foundation Grants #2018305 and #2022139 awarded to L.T. and E.B.-Y.

Author affiliations: [a]Department of Anthropology, Wichita State University, Wichita, KS 67260; [b]Department of Archaeology and Ancient Near Eastern Cultures, Tel Aviv University, Tel Aviv 6997801, Israel; [c]Geosciences Research Division, Scripps Institution of Oceanography, University of California San Diego, La Jolla, CA 92093; [d]Digital Pasts Lab, Department of Land of Israel Studies and Archaeology, Social Sciences and Humanities, Ariel University, Ariel 40700, Israel; [e]Geosciences Research Division, Digital Humanities and Social Sciences Hub, Open University, Ra'anana 4353701, Israel; [f]Geosciences Research Division, Institute of Archaeology, University College London, London WC1E 6BT, United Kingdom; and [g]Geosciences Research Division, University of Liverpool, Liverpool L69 3BX, United Kingdom

1. L. Néel, Influence des fluctuations thermiques sur l'aimantation de grains ferromagnétiques très fins. *C. R. Hebd. Séances Acad. Des Sci.* **228**, 664–666 (1949).
2. E. Thellier, Sur l'aimantation des terres cuites et ses applications géophysique. *Ann. Inst. Phys. Globe Univ. Paris* **16**, 157–302 (1938).
3. J. G. Koenigsberger, Natural residual magnetism of eruptive rocks. *Terr. Magnet. Atmos. Electr.* **43**, 299–320 (1938).
4. E. Ben-Yosef, L. Tauxe, T. E. Levy, Archaeomagnetic dating of copper smelting site F2 in the Timna Valley (Israel) and its implications for the modelling of ancient technological developments. *Archaeometry* **52**, 1110–1121 (2010).
5. G. Hervé *et al.*, How did the dipole axis vary during the first millennium BCE? New data from West Europe and analysis of the directional global database. *Phys. Earth Planet. Int.* **315**, 106712 (2021).
6. F. J. Pavón-Carrasco, M. L. Osete, J. M. Torta, A. De Santis, A geomagnetic field model for the Holocene based on archaeomagnetic and lava flow data. *Earth Planet. Sci. Lett.* **388**, 98–109 (2014).
7. C. Constable, M. Korte, S. Panovska, Persistent high paleosecular variation activity in southern hemisphere for at least 10,000 years. *Earth Planet Sci. Lett.* **453**, 78–86 (2016).
8. M. L. Osete *et al.*, Two archaeomagnetic intensity maxima and rapid directional variation rates during the Early Iron Age observed at Iberian coordinates. Implications on the evolution of the Levantine Iron Age Anomaly. *Earth Planet. Sci. Lett.* **533**, 116047 (2020).
9. E. Ben-Yosef *et al.*, Application of copper slag in geomagnetic archaeointensity research. *J. Geophys. Res. Solid Earth* **113**, B08101 (2008).
10. R. Shaar *et al.*, Archaeomagnetism in the Levant and Mesopotamia reveals the largest changes in the geomagnetic field. *J. Geophys. Res. Solid. Earth* **127**, e2022JB024962 (2022).
11. E. Ben-Yosef *et al.*, Geomagnetic intensity spike recorded in high resolution slag deposit in Southern Jordan. *Earth Planet Sci. Lett.* **287**, 529–539 (2009).
12. R. Shaar *et al.*, Geomagnetic field intensity: How high can it get? How fast can it change? Constraints from Iron Age copper slag. *Earth Planet. Sci. Lett.* **301**, 297–306 (2011).
13. Y. Yu, L. Tauxe, A. Genevey, Toward an optimal geomagnetic field intensity determination technique. *Geochem. Geophys. Geosyst.* **5**, Q02H07 (2004).
14. R. Shaar, L. Tauxe, Thellier GUI: An integrated tool for analyzing paleointensity data from Thellier-type experiments. *Geochem. Geophys. Geosyst.* **14**, 677–692 (2013).
15. M. C. Brown *et al.*, GEOMAGIA50. v3: 1. General structure and modifications to the archeological and volcanic database. *Earth, Planets Space* **67**, 1–31 (2015).
16. R. Shaar *et al.*, Synchronizing geomagnetic field intensity records in the levant between the 23rd and 15th centuries BCE: Chronological and methodological implications. *Geochem. Geophys. Geosyst.* **21**, e2020GC009251 (2020).
17. A. Genevey, Y. Gallet, J. Margueron, Eight thousand years of geomagnetic field intensity variations in the eastern Mediterranean. *J. Geophys. Res. Solid Earth* **108**, 2228 (2003).
18. P. Ertepinar *et al.*, Archaeomagnetic study of five mounds from Upper Mesopotamia between 2500 and 700 BCE: Further evidence for an extremely strong geomagnetic field ca. 3000 years ago. *Earth Planet. Sci. Lett.* **357**, 84–98 (2012).
19. Y. Gallet, M. Le Goff, High-temperature archeointensity measurements from Mesopotamia. *Earth Planet. Sci. Lett.* **241**, 159–173 (2006).
20. Y. Gallet, A. Genevey, M. Le Goff, F. Fluteau, S. A. Eshraghi, Possible impact of the Earth's magnetic field on the history of ancient civilizations. *Earth Planet Sci. Lett.* **246**, 17–26 (2006).
21. Y. Gallet, P. Butterlin, Archaeological and geomagnetic implications of new archaeomagnetic intensity data from the early bronze high terrace 'Massif Rouge' at Mari (Tell Hariri, Syria). *Archaeometry* **57**, 263–276 (2015).
22. M. D. Stillinger, J. M. Feinberg, E. Frahm, Refining the archaeomagnetic dating curve for the Near East: New intensity data from Bronze Age ceramics at Tell Mozan, Syria. *J. Archaeolog. Sci.* **53**, 345–355 (2015).
23. Y. Gallet, M. Le Goff, A. Genevey, J. Margueron, P. Matthiae, Geomagnetic field intensity behavior in the Middle East between ~3000 BC and ~1500 BC. *Geophys. Res. Lett.* **35**, 17–26 (2008).
24. Y. Gallet, M. Fortin, A. Fournier, M. Le Goff, P. Livermore, Analysis of geomagnetic field intensity variations in Mesopotamia during the third millennium BC with archeological implications. *Earth Planet. Sci. Lett.* **537**, 116183 (2020).
25. M. J. Aitken, A. L. Allsop, G. D. Bussell, M. B. Winter, Geomagnetic intensity in Egypt and western Asia during the second millennium BC. *Nature* **310**, 305–306 (1984).
26. H. Sakai, "Variation of geomagnetic field deduced from analysis of remanent magnetization of archaeological objects," PhD dissertations, Osaka University, Osaka, Japan (1980).
27. D. Walton, The intensity of the geomagnetic field in the eastern Mediterranean between 1600 BC and AD 400. *J. Geomagnet. Geoelectr.* **42**, 929–936 (1990).
28. Y. Vaknin *et al.*, The Earth's magnetic field in Jerusalem during the Babylonian destruction: A unique reference for field behavior and an anchor for archaeomagnetic dating. *PLoS One* **15**, e0237029 (2020).
29. P. Ertepinar *et al.*, Extreme geomagnetic field variability indicated by Eastern Mediterranean full-vector archaeomagnetic records. *Earth Planet. Sci. Lett.* **531**, 115979 (2020).
30. M. Korte, C. G. Constable, Archeomagnetic intensity spikes: Global or regional geomagnetic field features? *Front. Earth Sci.* **6**, 17 (2018).
31. R. Shaar, L. Tauxe, A. Goguitchaichvili, M. Devidze, V. Licheli, Further evidence of the Levantine Iron Age geomagnetic anomaly from Georgian pottery. *Geophys. Res. Lett.* **44**, 2229–2236 (2017).
32. M. M. Kovacheva, M. Kostadinova-Avramova, N. Jordanova, P. Lanos, Y. Boyadzhiev, Extended and revised archaeomagnetic database and secular variation curves from Bulgaria for the last eight millennia. *Phys. Earth Planet. Int.* **236**, 79–94 (2014).
33. M. Rivero-Montero *et al.*, Geomagnetic field intensity changes in the Central Mediterranean between 1500 BCE and 150 CE: Implications for the Levantine Iron Age Anomaly evolution. *Earth Planet. Sci. Lett.* **557**, 116732 (2021).
34. N. García-Redondo *et al.*, Further evidence of high intensity during the Levantine Iron Age Anomaly in southwestern Europe: Full vector archeomagnetic dating of an Early Iron Age dwelling from Western Spain. *J. Geophys. Res. Solid. Earth* **126**, e2021JB022614 (2021).
35. A. Molina-Cardín *et al.*, Updated Iberian archeomagnetic catalogue: New full vector paleosecular variation curve for the last three millennia. *Geochem. Geophys. Geosyst.* **19**, 3637–3656 (2018).
36. C. Kissel *et al.*, Holocene geomagnetic field intensity variations: Contribution from the low latitude Canary Islands site. *Earth Planet. Sci. Lett.* **430**, 178–190 (2015).
37. A. Di Chiara *et al.*, Constraining chronology and time-space evolution of Holocene volcanic activity on the Capelo Peninsula (Faial Island, Azores): The paleomagnetic contribution. *GSA Bull.* **126**, 1164–1180 (2014).
38. S. Cai *et al.*, Archaeointensity results spanning the past 6 kiloyears from eastern China and implications for extreme behaviors of the geomagnetic field. *Proc. Natl. Acad. Sci. U.S.A.* **114**, 39–44 (2017).
39. C. Davies, C. Constable, Geomagnetic spikes on the core-mantle boundary. *Nat. Commun.* **8**, 15593 (2017).
40. F. J. Pavón-Carrasco *et al.*, SCHA.DIF.4k: 4,000 years of paleomagnetic reconstruction for Europe and its application for dating. *J. Geophys. Res. Solid. Earth* **126**, e2020JB021237 (2021).
41. A. Di Chiara *et al.*, An archaeomagnetic study of the Ishtar Gate, Babylon, *PLoS One*, in press.
42. L. Tauxe, R. Shaar, B. Cych, E. Ben-Yosef, "Uncertainties in archaeointensity research: Implications for the levantine archaeomagnetic curve" in *And in length of days understanding (Job 12:12)*, E. Ben-Yosef, I. W. N. Jones, Eds. (*Interdisciplinary Contributions to Archaeology*, Springer Nature, 2023).
43. G. Algaze, *Ancient Mesopotamia at the dawn of civilization: The evolution of an urban landscape* (University of Chicago Press, 2008).
44. E. Hammer, Multi-centric, Marsh-based Urbanism at the early Mesopotamian city of Lagash (Tell al-Hiba, Iraq). *J. Anthropol. Archaeol.* **68**, 101458 (2022).
45. R. Pruzsinszky, *Mesopotamian Chronology of the 2nd Millenium B.C.: An Introduction to the Textual Evidence and Related Chronological Issues* (*Contributions to the Chronology of the Eastern Mediterranean*, Verlag der Österreichischen Akademie der Wissenschaften, 2009), p. 227.
46. A. Salonen, *Die Ziegeleien im Alten Mesopotamien* (Academia Scientiarum Fennica, 1972).
47. D. Oates, Innovations in mud-brick: Decorative and structural techniques in ancient Mesopotamia. *World Archaeol.* **21**, 388–406 (1990).
48. U. Finkbeiner, "Uruk-Warka, Evidence of the Gamdat Nasr Period," in *Gamdat Nasr: Period or Regional Style?: Papers Given at a Symposium Held in Tübingen*, November 1983., U. Finkbeiner, W. Röllig, Eds. (Reichert, 1986), pp. 33–56.
49. P. R. S. Moorey, *Ancient Mesopotamian Materials and Industries: The Archaeological Evidence* (Eisenbrauns, 1994).
50. S. Bertman, *Handbook to Life in Ancient Mesopotamia* (Oxford University Press, 2005).
51. G. R. H. Wright, *Ancient Building Technology, Volume 1: Historical Background* (Brill, 2000).
52. H. Frankfort, *Town Planning in Ancient Mesopotamia* (University of Liverpool, 1950).
53. C. B. F. Walker, *Cuneiform Brick Inscriptions* (British Museum Pub, 1981).
54. M. Sauvage, "Mathematical computations in the management of public construction work in Mesopotamia (End of the third and beginning of the second millennium BCE)" in *Mathematics, Administrative and Economic Activities in Ancient Worlds*, C. Michel, K. Chemla, Eds. (Springer International Publishing, 2020), pp. 201–237.
55. P. Huber, "Dating by month-lengths revisited" in *Studies on the Ancient Exact Sciences in Honour of Lis Brack-Bernsen*, J. Steele, M. Ossendrijver, Eds. (Excellence Cluster Topoi, 2017), pp. 19–68.

56. F. Höflmayer, S. W. Manning, A synchronized early Middle Bronze Age chronology for Egypt, the Levant, and Mesopotamia. *J. Near East. Stud.* **81**, 1–24 (2022).
57. J. Jeffers, The nonintercalated lunar calendar of the middle assyrian period. *J. Cuneiform Stud.* **69**, 151–191 (2017).
58. C. Michel, P. Rocher, La Chronologie du lie millénaire revue ä l'ombre d'une éclipse de soleil. *Jaarbericht Ex Oriente Lux* **35**, 111–126 (2000).
59. J. Mebert, Die Venustafeln des Ammī-á¹£aduqa und ihre Bedeutung für die astronomische Datierung der altbabylonischen Zeit (Archiv für Orientforschung Beiheft 31, Institut für Orientalistik, 2011).
60. H. Gasche, J. A. Armstrong, S. W. Cole, V. G. Gurzadyan, *Dating the Fall of Babylon: A Reappraisal of Second-Millenium Chronology* (*Mesopotamian History and Environment, Series II*, University of Ghent and the Oriental Institute of the University of Chicago, Chicago, 1998). vol. Memoirs 4.
61. J. A. Brinkman, *Mesopotamian Chronology of the Historical Period* (University of Chicago Press, 2021).
62. K. Radner, Cuneiform inscriptions in the Archaeological Museum of Sulaimaniya. *Archiv für Orientforschung* **52**, 98–103 (2011).
63. A. K. Grayson, *Assyrian Rulers of the Third and Second Millennia BC (to 1115 BC)* (University of Toronto Press, 2016).
64. V. Donbaz, A. K. Grayson, *Royal Inscriptions on Clay Cones from Ashur Now in Istanbul* (University of Toronto Press, 1984).
65. D. Frayne, *Old Babylonian Period (2003-1595 B.C.): Early Periods, Volume 4* (University of Toronto Press, Toronto, ON, 1990).
66. B. Cych, M. Morzfeld, L. Tauxe, Bias Corrected Estimation of Paleointensity (BiCEP): An improved methodology for obtaining paleointensity estimates. *Geochem. Geophys. Geosyst.* **22**, e2021GC009755 (2021).
67. P. W. Livermore, Y. Gallet, A. Fournier, Archeomagnetic intensity variations during the era of geomagnetic spikes in the Levant. *Phys. Earth Planet. Int.* **312**, 106657 (2021).
68. E. Thellier, O. Thellier, Sur l'intensité du champ magnétique terrestre dans le passé historique et géologique. *Ann. Geophys.* **15**, 285–376 (1959).
69. R. S. Coe, The determination of paleo-intensities of the Earth's magnetic field with emphasis on mechanisms which could cause non-ideal behavior in Thellier's method. *J. Geomagnet. Geoelectr.* **19**, 157–179 (1967).
70. L. Tauxe *et al.*, PmagPy: Software package for paleomagnetic data analysis and a bridge to the Magnetics Information Consortium (MagIC) Database. *Geochem. Geophys. Geosyst.* **17**, 2450–2463 (2016).
71. V. P. Shcherbakov, F. Lhuillier, N. K. Sycheva, Exact analytical solutions for kinetic equations describing thermochemical remanence acquisition for single-domain grains: Implications for absolute paleointensity determinations. *J. Geophys. Res. Solid. Earth* **126**, e2020JB021536 (2021).
72. G. A. Paterson, A simple test for the presence of multidomain behavior during paleointensity experiments. *J. Geophys. Res. Solid Earth* **116**, B10104 (2011).
73. L. Tauxe *et al.*, Software package for paleomagnetic data analysis and a bridge to the Magnetics Information Consortium (MagIC) Database. PmagPy. https://github.com/PmagPy/PmagPy. Deposited 23 February 2016.
74. B. Cych, M. Morzfeld, L. Tauxe, Bias Corrected Estimation of Paleointensity (BiCEP): an improved methodology for obtaining paleointensity estimates. BiCEP. https://github.com/bcych/BiCEP_GUI. Deposited 28 June 2023.
75. M. D. Howland *et al.*, Magnetics Information Consortium. MagIC. https://earthref.org/MagIC/19893. Deposited 16 June 2023.
76. M. D. Howland *et al.*, Mesopotamian Brick Orthophotos and Editions. GitHub. https://github.com/DigitalPasts/BricksGeomagnetism. Deposited 27 July 2023.
77. M. D. Howland *et al.*, Magnetics Information Consortium. MagIC. https://earthref.org/MagIC/19893/d4b397b9-f200-479f-8cbf-1492e3df910b. Deposited 27 July 2023.